

## Holographic Recording and Control of Diffraction Efficiency Using Photoinduced Surface Deformation on Azo-Polymer Films

Kenji HARADA\*, Hajime INOUE, Mohamed A. EL-MORSY<sup>1</sup>, Masahide ITOH, Shinsuke UMEGAKI<sup>2</sup> and Toyohiko YATAGAI

*Institute of Applied Physics and Tsukuba Advanced Research Alliance (TARA), University of Tsukuba, Tsukuba 305-8573, Japan*

<sup>1</sup>*Physics Department, Faculty of Science, Damietta, University of Mansoura, Damietta, Egypt*

<sup>2</sup>*Faculty of Science and Technology, Keio University, Hiyoshi, Yokohama 223-0061, Japan*

(Received October 1, 2001; accepted for publication October 30, 2001)

Surface relief holograms were fabricated on azo-polymer films by the irradiation of interference laser fringes. The side-chain azo-polymer, poly-orange tom-1 isophoronediiisocyanate, was used in this study. Recording characteristics of surface relief structures were investigated; they needed no post-treatment, and could be erased by heating or irradiating a uniform laser beam. The diffraction efficiency of the recorded hologram was markedly increased by corona charging. It was also controlled by irradiation of the laser beam (488 nm) with corona charging. [DOI: 10.1143/JJAP.41.1851]

KEYWORDS: hologram, azo-polymer, photoinduced surface deformation, surface relief grating, corona charging

### 1. Introduction

Polymeric materials are the most promising organic materials for electrooptic devices and memory devices. The recording of polarization holographic gratings using azobenzene-containing polymer films as photoanisotropic materials has been reported.<sup>1)</sup> This photoinduced anisotropic effect is due to trans-cis-trans isomerization and the orientational effects of the azo-dye chromophore. Direct fabrication of relief structures in azo-polymers has been reported in the past several years.<sup>2–5)</sup> A surface relief structure is recorded through photoisomerization and the movements of the polymer chains.<sup>6,7)</sup> This is a one-step fabrication technique. A surface relief structure is fabricated by irradiation of interference laser fringes onto azobenzene functionalized polymers such as side-chain-type and main-chain-type azo-polymers. The diffraction efficiency and the surface relief depth depend on the writing energy and the polarization of the writing laser beam.<sup>8)</sup> This structure is very stable at temperatures below the glass transition temperature  $T_g$  and can be erased by heating above  $T_g$ . This fabrication mechanism is not well understood at present, but several models have been proposed.<sup>9–12)</sup>

We have recently reported that the diffraction efficiency of the surface relief structure can be markedly increased by corona charging.<sup>13)</sup> Moreover, such a hologram exhibits non-linearity, because the orientation of the azo chromophore and the increase in the diffraction efficiency are performed concurrently by corona charging. Surface relief grating fabrication and the modulation of a surface relief electrooptic grating have been reported.<sup>14)</sup>

In this paper, surface relief holograms are fabricated on azo-polymer films by irradiation of interference laser fringes. The diffraction efficiency of the hologram is controlled by irradiation of the laser beam with corona charging.

### 2. Surface Deformation Method

The side-chain azo-polymer, poly-orange tom-1 isophoronediiisocyanate, is used in this study. Figure 1 shows the chemical structure and absorption spectrum of the mate-

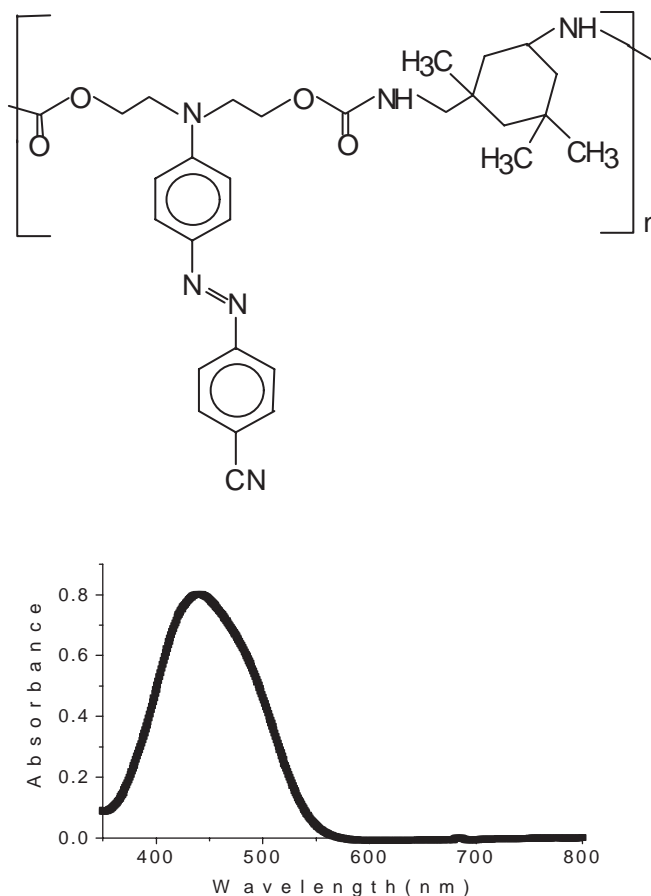


Fig. 1. Chemical structure and absorption spectrum of the material.

rial. The glass transition temperature is 136°C. The absorption peak and the cut-off wavelength of the dye are 440 nm and 560 nm, respectively. This polymer is dissolved in cyclohexanone. Samples of 1–5  $\mu\text{m}$  thickness are prepared by spin-coating on a slide glass plate. The refractive index of the film is measured as 1.65 at a wavelength of 633 nm by the m-line technique.

The surface relief grating is fabricated by the irradiation of two-beam interference fringes. The experimental setup is

\*E-mail address: harada@optlab2.bk.tsukuba.ac.jp

shown in Fig. 2. A polarized Ar-ion laser beam at a wavelength of 488 nm is used as the light source. The laser beam is collimated to 6 mm in diameter, half of the laser beam is reflected by a mirror and the two beams interfere on the sample. The setup is strong arrangement in the vibration. The angle between the sample and the mirror is  $90^\circ$  and the period of the grating can be adjusted by varying the angle between  $\theta$  the beam propagation axis and the mirror plane. Figure 3 shows the polarization dependence of the diffraction efficiency. The period of the surface relief grating is selected as  $1 \mu\text{m}$ . There is a strong polarization dependence of the writing laser beam. High diffraction efficiency is obtained using a p- or circularly polarized writing beam. The relief structure is not recorded using an s-polarized writing beam. A high diffraction efficiency can be obtained in a short time by high-power recording.<sup>13)</sup> Figure 4 shows an atomic force microscopy image of

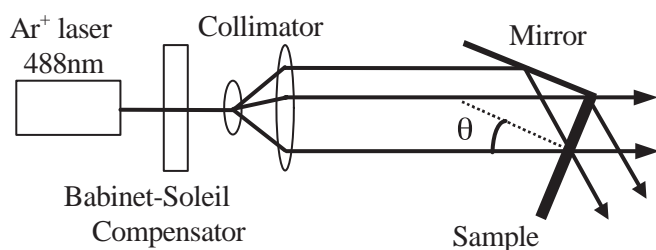


Fig. 2. Optical setup for surface relief grating fabrication by the surface deformation method.

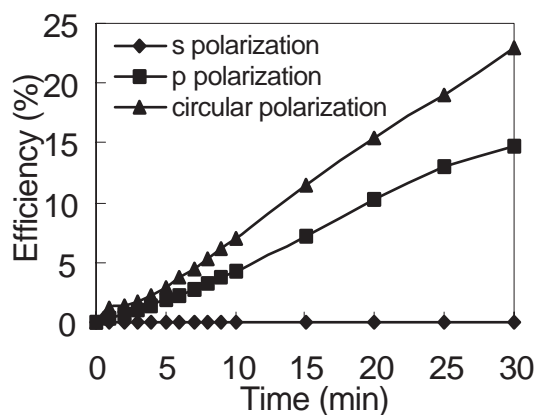


Fig. 3. Polarization dependence of the diffraction efficiency.

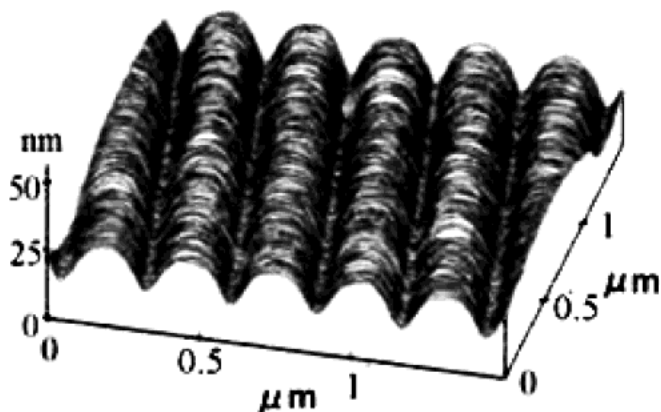


Fig. 4. Atomic force microscopy image of surface relief structure.

a surface relief structure recorded using a p-polarized beam. The laser beam power was  $220 \text{ mW/cm}^2$  for 10 min. A minimum relief period of  $275 \text{ nm}$  was recorded. The surface relief depth was  $16 \text{ nm}$ .

### 3. Recording of Fourier Transform Hologram

Next, we examined Fourier transform hologram recording using the photoinduced surface modulation technique. The hologram recording setup is shown in Fig. 5. A circularly polarized Ar-ion laser beam with a wavelength of 488 nm was used. The laser beam was collimated to a 6 mm diameter and separated by a beam splitter. The Fourier transform hologram was recorded on an azo-polymer film with a thickness of about  $2 \mu\text{m}$ . The letter A, 4 mm tall and 3 mm wide, was used as the object. The beam power in front of the object was  $I_1 = 118 \text{ mW/cm}^2$ . The object beam was Fourier transformed on the azo-polymer film using a lens with a focal length of 100 mm. The reference beam power was  $I_2 = 118 \text{ mW/cm}^2$  and the recording time was 1 min. The reconstructed image is shown in Fig. 6(a). This reconstructed image was observed using a He-Ne laser beam. The diffraction efficiency of the recorded hologram measured using a He-Ne laser was 1.2%.

### 4. Diffraction Efficiency Control of the Hologram

We have recently confirmed that the diffraction efficiency and the relief depth of a surface relief structure is markedly increased by corona charging at temperatures near or above its  $T_g$ .<sup>13)</sup> The mechanism is not clearly understood, but we consider that the relief depth increases as a result of the Coulomb force exerted by electric charge; therefore the diffraction efficiency is increased. This increase depends on the corona

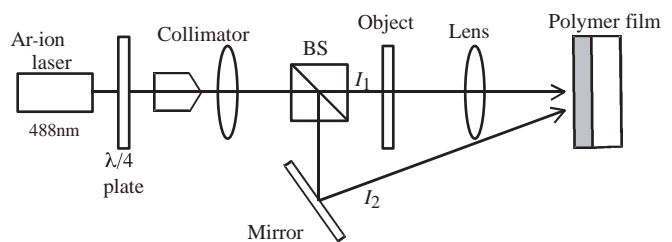


Fig. 5. Experimental setup for Fourier transform hologram recording.

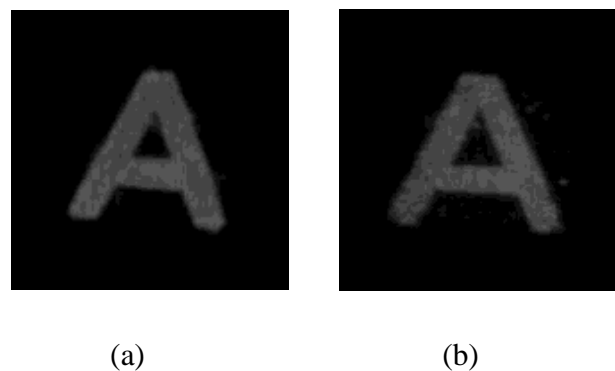


Fig. 6. The reconstructed images (a) before corona charging and (b) after corona charging.

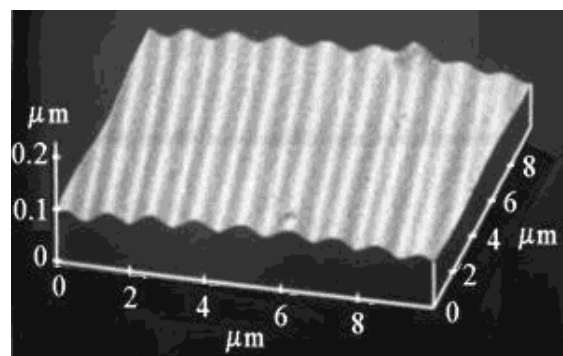
charging conditions, specifically, the corona charging temperature, the applied voltage and the corona charging time. The increase can be used to increase the initially low diffraction efficiency of the recorded hologram. We examined the increase in diffraction efficiency of the letter A recorded by the Fourier transform hologram. The Fourier transform hologram was recorded using the hologram recording setup shown in Fig. 5. The recording power and time were  $I_1 = I_2 = 88 \text{ mW/cm}^2$  and 1 min, respectively. The period of interference fringes was  $1 \mu\text{m}$ .

The electric charge was deposited on the hologram using a corona deposition poling setup in an oven. A sharp needle electrode was positioned above the ground electrodes. The hologram was placed on the ground electrode. The distance between the polymer film and the needle electrode was 7 mm.

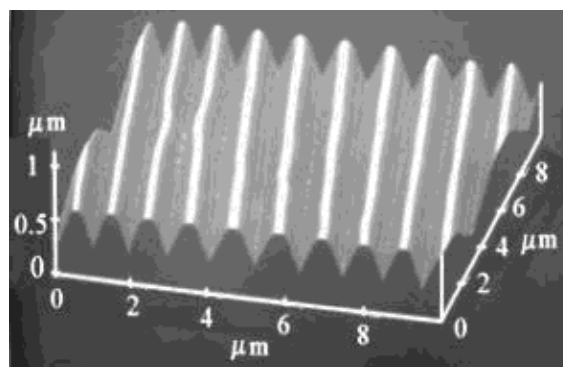
In the corona charging process, the voltage was applied at a temperature near  $T_g$  and the polymer film was heated to the corona charging temperature with the voltage applied, because the surface relief structure is thermally erased above  $T_g$  without the applied voltage. After corona charging for 20 min, the polymer film was cooled to room temperature with the applied voltage. During the corona charging process, a voltage of 7 kV was applied at  $141^\circ\text{C}$ . The first-order diffraction efficiency of the hologram measured before and after corona charging using a He-Ne laser increased from 0.24% to 28.39%. This increase in the corona charging depends on the corona charging conditions, and the increase in the diffraction efficiency of the hologram can be controlled by these conditions. The reconstructed images after corona charging are shown in Fig. 6(b).

We observed the recorded Fourier transform hologram using an atomic force microscope (AFM). The surface profiles of the Fourier transform hologram before and after corona charging are shown in Figs. 7(a) and 7(b). The relief depths measured before and after corona charging were about 20 nm and about 350 nm, respectively. This indicates that the increased diffraction efficiency caused by corona charging strongly depends on the increased relief depth of the recorded hologram. We have confirmed that the diffraction efficiency of the hologram increases markedly as a result of corona charging, and the maximum diffraction efficiency is over 30%. The first-order diffraction efficiency of the increased Fourier hologram remained unchanged for several months at room temperature under natural light.

Next, the diffraction efficiency was controlled by the irradiation of the laser beam. A circularly polarized laser beam was irradiated onto the hologram with corona charging at  $141^\circ\text{C}$ . The reflected first-order diffraction efficiency of the He-Ne laser was detected. Figure 8 shows the *in situ* measurement of the diffraction efficiency control of the hologram. At  $t = 0 \text{ s}$ , the electric charge was deposited on the hologram at  $130^\circ\text{C}$ . The applied voltage was 6.5 kV. At  $t = 20 \text{ s}$ , the hologram was heated to  $150^\circ\text{C}$  with corona charging. Diffraction efficiency increased upon heating the sample to above its  $T_g$  with corona charging. At  $t = 90 \text{ s}$ , a uniform Ar-ion laser beam of about  $5 \text{ mW/cm}^2$  was irradiated onto the hologram. The increase in the diffraction efficiency became slower. At  $t = 130 \text{ s}$ , uniform Ar-ion laser beam of about  $50 \text{ mW/cm}^2$  was irradiated onto the hologram and the diffraction efficiency decreased. At  $t = 150 \text{ s}$ , the Ar-ion laser beam was



(a)



(b)

Fig. 7. Surface profiles of the Fourier transform hologram (a) before corona charging and (b) after corona charging.

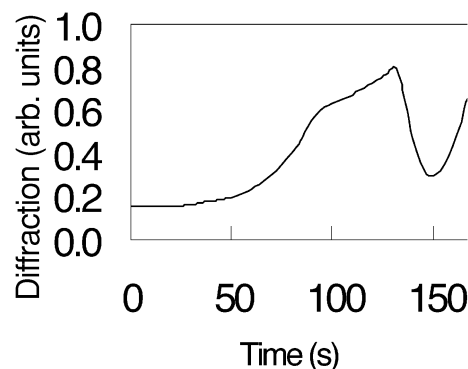


Fig. 8. Diffraction efficiency control of the hologram.

turned off and the diffraction efficiency increased again.

Thus, the diffraction efficiency was increased by the corona charging, and decreased by the laser beam irradiation with corona charging. We can control the diffraction efficiency of the surface relief hologram by controlling the irradiation power of the laser beam. To our knowledge, this is the first example of diffraction efficiency control of a surface relief hologram by the irradiation of a laser beam with corona discharge.

## 5. Conclusions

We proposed a new hologram recording technique using photoinduced surface deformation on azo-polymer films. The first-order diffraction efficiency of the hologram increased from 0.24% to 28.39%. The diffraction efficiency was controlled by the irradiation of a uniform laser beam at a wavelength of 488 nm with corona charging. This recording technique can be applied to holographic memory devices.

## Acknowledgments

This research was partly supported by a Grant-in-Aid for Scientific Research from the Ministry of Education, Culture, Sports, Science and Technology and by the Yatagai Project, Tsukuba Advanced Research Alliance, University of Tsukuba.

- 1) K. Kawano, T. Ishii, J. Minabe, T. Niitsu, Y. Nishikata and K. Baba: *Opt. Lett.* **24** (1999) 1269.
- 2) D. Y. Kim, L. Li, X. L. Jiang, V. Shivshankar, J. Kumar and S. K.

- Tripathy: *Macromolecules* **28** (1995) 8835.
- 3) C. J. Barrett, A. L. Natansohn and P. L. Rochon: *J. Phys. Chem.* **100** (1996) 8836.
- 4) N. C. R. Holme, L. Nikolva, P. S. Ramanujam and S. Hvilsted: *Appl. Phys. Lett.* **70** (1997) 1518.
- 5) M. Itoh, K. Harada, H. Matsuda, S. Ohnishi, A. Parfenov, N. Tamaoki and T. Yatagai: *J. Phys. D: Appl. Phys.* **31** (1998) 463.
- 6) C. J. Barrett, P. L. Rochon and A. L. Natansohn: *J. Chem. Phys.* **109** (1998) 1505.
- 7) D. Y. Kim, S. K. Tripathy, L. Li and J. Kumar: *Appl. Phys. Lett.* **66** (1995) 1166.
- 8) X. L. Jiang, L. Li, J. Kumar, D. Y. Kim, V. Shivshankar and S. K. Tripathy: *Appl. Phys. Lett.* **68** (1996) 2618.
- 9) T. G. Pedersen, P. M. Johansen, N. C. R. Holm, P. S. Ramanujam and S. Hvilsted: *Phys. Rev. Lett.* **80** (1997) 89.
- 10) J. Kumar, L. Li, X. L. Jiang, D. Y. Kim, T. S. Lee and S. Tripathy: *Appl. Phys. Lett.* **72** (1998) 2096.
- 11) C. J. Barrett, P. L. Rochon and A. L. Natansohn: *J. Chem. Phys.* **109** (1998) 1505.
- 12) K. Sumaru, T. Yamanaka, T. Fukuda and H. Matsuda: *Appl. Phys. Lett.* **75** (1999) 1878.
- 13) K. Munakata, K. Harada, H. Anji, M. Itoh, S. Umegaki and T. Yatagai: *Opt. Lett.* **26** (2001) 4.
- 14) K. Munakata, K. Harada, N. Yoshikawa, M. Itoh, S. Umegaki and T. Yatagai: *Opt. Rev.* **6** (1999) 518.